Published in final edited form as:
Neuroimage. 2010 October 1; 52(4): 1230–1237. doi:10.1016/j.neuroimage.2010.05.018.

STRUCTURAL CONNECTIVITY OF BROCA'S AREA AND MEDIAL FRONTAL CORTEX

Anastasia Ford[1,2,*], **Keith M. McGregor**[1,2], **Kimberly Case**[1,2], **Bruce Crosson**[1,3], and **Keith D. White**[1,2,3]

[1] Brain Rehabilitation Research Center, Malcom Randall VA Medical Center, Gainesville, FL 32608, USA

[2] Department of Psychology, University of Florida, Gainesville, FL 32611, USA

[3] Department of Clinical and Health Psychology, University of Florida, Gainesville, FL 32610, USA

Abstract

Despite over 140 years of research on Broca's area, the connections of this region to medial frontal cortex remain unclear. The current study investigates this structural connectivity using diffusion weighted MRI tractography in living humans. Our results show connections between Broca's area and Brodmann's areas (BA) 9, 8, and 6 (both supplementary motor area (SMA) in caudal BA 6, and Pre-SMA in rostral BA 6). Trajectories follow an anterior-to-posterior gradient, wherein the most anterior portions of Broca's area connect to BA 9 and 8 while posterior Broca's area connects to Pre-SMA and SMA. This anterior-posterior connectivity gradient is also present when connectivity-based parcellation of Broca's area is performed. Previous studies of language organization suggest involvement of anterior Broca's area in semantics and posterior Broca's area in syntax/phonology. Given corresponding patterns of functional and structural organization of Broca's area, it seems well warranted to investigate carefully how anterior vs. posterior medial frontal cortex differentially affect semantics, syntax and phonology.

Introduction

Despite over 140 years of research on Broca's area, the connections of this region to medial frontal cortex in human brain remain unclear. Classical views of language organization, based primarily on human brain lesions, have long implicated Broca's and Wernicke's areas as important cortical loci of language processing (Broca, 1861; Wernicke, 1874; Lichtheim, 1885). More recent studies have identified further cortical substrates, as well as subcortical structures, involved in language (Binder et al., 1997; Crosson et al., 1999; Crosson et al., 2007) building upon the development of functional neuroimaging techniques such as positron emission tomography and functional magnetic resonance imaging (fMRI). Many of these studies have identified regions that co-activate during language paradigms, and thus are thought to be members of the same functional network (Crosson et al., 2001; Horwitz et al., 1998). While functional connectivity as evidenced by co-activation implies the existence

[*]Corresponding author: Department of Psychology, University of Florida, P. O. Box 112250, Gainesville, FL 32611-2250, USA. Tel: (352) 273-2143, Fax: (352) 392-7985, sokolova@u.edu.

of a neural network, it does not define structural connectivity per se. Known structural connectivity of a given neural substrate can provide insight into the physiological mechanisms for network organization, as well as into potential functional characteristics.

Much of what is currently known about structural connectivity of human language areas comes indirectly from non-human primate literature. Comparative cytoarchitectonic studies have identified monkey homologues of human Broca's region, namely Brodmann's areas (BA) 44 and 45 (Petrides & Pandya, 1994; Petrides, 2005). In particular, using architectonic comparison and electrophysiological recordings and microstimulaiton, Petrides and colleagues found an area anterior to monkey area 44 involved with control of orafacial musculature (Petrides et al., 2005). The authors postulated that this area further developed to control communicative acts and eventually human speech in the progression of primate phylogeny. In addition, connectivity patterns of monkey BA 44/45 are distinct, implying differences in their functional domain. While area 44 is connected with the ventral premotor cortex, which has orofacial and hand/arm representations, BA 45 in monkey is connected to the superior temporal sulcus (STS). Further work by Petrides and Pandya demonstrated projections from this monkey analogue of Broca's region to the superior temporal gyrus (STG), the upper bank of STS (monkey analogues of human Wernicke's area), and also to the medial frontal cortex (Petrides & Pandya, 2002).

Projections from human BA 44/45 to the STG have been implied by a number of fMRI studies suggesting functional connectivity (Klein et al., 1995; Petrides, 1995; Binder et al., 1997) as well as by diffusion-weighted MRI (DW-MRI) suggesting structural connectivity (See Friederici et al 2009 for a comprehensive review). Recent studies employing applications of DW-MRI have provided many valuable insights into Broca's area connectivity. Catani and colleagues demonstrated direct as well as indirect connections between Broca's and Wernicke's areas serving phonological and semantic functions respectively (Catani et al., 2005). Glasser and Rilling divided the arcuate fasciculus into two segments: one originating in BA 44/45 and terminating in the posterior STG subserving phonology, and the other originating in BA 44/45 and BA 6/9 and terminating in the middle temporal gyrus (MTG) subserving lexical-semantic processing (Glasser & Rilling, 2008).

Functional connectivity of Broca's area with medial frontal cortex has been inferred from a number of fMRI studies (Crosson et al., 2001; Binkofski et al., 2000), as well as being strongly implied by the mirror-neuron theory of language (Rizzolatti & Craighero, 2004). Structural connectivity with the medial frontal cortex has been shown previously, although not studied extensively (Anwander et al., 2007, p. 820). Better understanding of the connectivity between these regions will provide valuable insights into language organization as it may relate to the selection and initiation of motor acts, and to mirror-neuron sensorimotor networks which are present in monkey BA 44/45 (Rizzolatti & Arbib, 1998). Clinically, the existence of these connections and knowledge about their trajectories could help to better predict language impairments and recovery after lesions involving Broca's area, or white matter in its vicinity or along these trajectories, or medial cortex to which Broca's area is connected. Understanding these connections also eventually can be useful in specifying the roles of medial frontal cortex in language functions. Medial frontal cortex has previously been implicated in action selection/outcome monitoring, behavioral adjustments, and learning (Ridderinkhof et al., 2004; Rushworth et al., 2004; Rushworth et al., 2007), all of which are important in complex cognitive tasks such as language. Monitoring selection and retrieval of grammatically correct and contextually appropriate responses, as well as adjusting behavioral output during a language task, would suggest a logical role for medial frontal cortex extending beyond classical language functions.

Structural connectivity between the monkey homologue of Broca's area and the medial frontal cortex has been previously demonstrated (Petrides & Pandya, 2002). To infer similar connectivity in humans, the present study identified analogous cortical regions in the medial frontal cortex as projection sites of Broca's area, namely BA 6 (caudally, as supplementary motor area (SMA); rostrally, as Pre-SMA), BA 8, and BA 9. The supracallosal BA 32 was included in the present analysis by extending the inferior boundary of the medial frontal masks to the cingulate sulcus. Because the paracingulate sulcus is absent in a large minority of humans, the borders between BA 8 or 6 and BA 32 are difficult to establish in those subjects (Crosson et al., 1999). Supracallosal BA 32 is thought to be equivalent to the cingulate motor areas in macaques. Because the cingulate motor areas in macaques have similar connectivity to their superior and adjacent counterparts in medial BA 6 (i.e., SMA, Pre-SMA), it seems reasonable to include BA 32 within the masks, although it is not specifically referenced in our naming conventions for these masks.

The present study employs DW-MRI to infer structural connectivity of human BA 44/45 specifically to medial frontal cortex. DW-MRI allows in-vivo visualization of white matter in the brain as inferred from the directional diffusion of water (Basser et al., 1994). The basic rationale is that, over a few tens of milliseconds, water molecules at normal physiological temperature can travel equal distances in any direction (i.e., isotropically) when they are in the middle of a large compartment like a ventricle, but can only travel more readily in select directions (i.e., anisotropically) if bounded by features impermeable to water like lipid cell membranes and myelin sheaths. Within a particular DW-MRI voxel, the preponderance of anisotropic over isotropic diffusion characterizes the voxel's fractional anisotropy (FA). The predominant direction of the anisotropic diffusion characterizes the voxel's principal eigenvector (PE). The quantities of FA and PE are determined by fitting a smooth tensor to DW-MRI data obtained by indexing diffusion along many directions. When PEs having nearly the same direction align or seemingly connect across contiguous voxels, they form a streamline suggestive of a tract.

The present study inferred tracts originating in BA 44/45 using probabilistic tractography, a fiber-tracking algorithm that provides better visualization of branching and crossing fibers than does a more traditional streamlining algorithm, and it also generates empirical likelihood estimates associated with the inferred tracts (Behrens et al., 2007). We also parcellated Broca's area using voxelwise likelihoods of connections originating in BA 44/45 and connecting to each of the aforementioned regions of medial cortex (Behrens et al., 2003b; Anwander et al., 2007). Probabilistic tractography enabled us to visualize trajectories of projection between Broca's area and regions in the medial frontal cortex, while connectivity-based segmentation allowed us to segment Broca's area based on the likelihood of connection to each of the four targets.

Methods

Participants

Nine right-handed, native English speakers, with no reported neurological disorders were recruited. Table 1 shows gender, age, and education level for each participant. Three out of nine of our participants were in the age range of 22 to 32 (mean = 26.3, st.dev. = 5.13) and will be referred to as younger participants. Six out of nine of our participants were in the age range of 64 to 82 (mean = 72.67, st.dev. = 7.74) and will be referred to as older participants. Written informed consent was obtained from all participants in compliance with Institutional Review Board guidelines of the University of Florida and the North Florida/South Georgia Malcom Randall Veteran's Affairs Medical Center.

Image Acquisition

All scans were obtained for each participant on a Philips Achieva 3T scanner (Amsterdam, Netherlands) using an 8-channel SENSE head coil. After a three-plane localizer scout used to center the fields of view to the participant's brain, and a field sensitivity reference scan for SENSE image reconstruction, a structural MP-RAGE T1-weighted scan was acquired with 130 × 1.0 mm sagittal slices, FOV = 240 mm (AP) × 180 mm (FH), matrix = 256 × 192, TR = 9.90 ms, TE = 4.60 ms, FA = 8 degrees, voxel size = 1.0 mm × 0.94 mm × 0.94 mm,, and time of acquisition = 6 min 11 sec. Diffusion-weighted images were acquired using single shot spin-echo echo planar imaging (EPI) with 60 × 2.0 mm axial slices (no gap), FOV = 224 mm (AP) × 224 mm (RL), matrix = 112 × 112, TR = 9509 ms, TE=55 ms, FA = 90 degrees, voxel size = 2.0 × 2.0 × 2.0 mm, and time of acquisition = 5 min 42 sec.. The diffusion weighing gradients were isotropically distributed in space using a 33-direction acquisition scheme with b=1000 s/mm2. A single volume with no diffusion weighting (b=zero) was also acquired with these parameters.

Data Analysis

Data processing was performed using the FSL software package FMRIB software Library (www.fmrib.ox.ac.uk/fsl). First, the eddy current distortions were removed (FDT, version 2.0), then each diffusion direction volume was registered to the b=zero volume using FLIRT (Jenkinson & Smith, 2001). Next, a binary mask of brain-only voxels was generated from the b=zero volume (Smith, 2002). The structural scans of each participant were skull stripped (Smith, 2002) and then registered to the participant's diffusion space (Jenkinson & Smith, 2001).

The tensor fit was performed in brain-only diffusion voxels (Behrens et al, 2003a). The fractional anisotropy (FA) and the principle eigenvector (PE) maps were examined to ensure proper fit and absence of distortions. Next, distributions of diffusion parameters, such as in-voxel fiber orientation, were estimated by running Markov Chain Monte Carlo (MCMC) sampling in each brain-only diffusion voxel (Behrens et al., 2007). Probabilistic tractography used these distributions to infer tracts connecting the seed voxels of interest in Broca's area to the targets in medial frontal cortex.

Tractography

Inferred fibers connecting voxels defined by a Broca's area seed mask to each of the medial frontal cortex target masks were visualized (Behrens et al, 2007). Details of the masks are given below. This tracking algorithm first estimates voxelwise probability density distributions for each parameter of the two-compartment simple partial volume model of diffusion, modeling 2 crossing fibers per voxel (Behrens et al., 2007) using MCMC. The two-compartment model assumes that all of the anisotropy in a given voxel comes from the presence of an inferred fiber, whereas all isotropic components would come from water surrounding the fiber. MCMC empirically estimates probability densities associated with inferred fiber orientations by drawing 1000 samples from each diffusion voxel. Highly anisotropic voxels support narrow orientation distributions and more isotropic voxels support broader distributions, thus no FA threshold is required. The tracking algorithm then calculates 5000 probabilistic streamlines, starting from each diffusion voxel within the seed mask, using step length of 0.5 mm (four steps per voxel), and utilizing the probability density of local fiber orientations in each voxel encountered along each streamline. Higher local probabilities in adjacent voxels for the particular fiber orientation that connects them (within a certain tolerance for curvature) will yield a large expected value for the number of associated streamlines passing through them, in contrast to a low expected value if the most probable orientations in these voxels are discrepant. We used a curvature threshold of 0.2,

which is the cosine of the allowable angle between two steps, as the tolerance parameter of the tracking algorithm.

The number of streamlines traversing each seed-to-target connection provides an empirical index concatenating the local orientation distributions of all the voxels traversed by those streamlines. Accumulating these indices for each target across voxels contained in the seed mask yields a connectivity distribution. Connectivity distributions for each of the medial frontal areas of interest represent how many probabilistic streamlines originated in voxels contained by the Broca's area seed mask, and reached voxels within each of the medial frontal target masks. Seed voxels having 10 or fewer out of 5000 possible streamlines connected to the target mask were found to be spatially disbursed away from the high connectivity voxel clusters of each connectivity distribution and were, therefore, attributed to noise and excluded from further analysis (see Ciccarelli et al., 2006 and Heiervang et al., 2006 for similar approach).

Connectivity-based Parcellation

After such exclusions, four sub-regions of interest became evident within the Broca's area (BA 44/45) seed mask. We performed a classification target analysis using the same four target masks to compute the likelihoods of connection between each voxel in the Broca's area mask and each of the four medial frontal targets (Behrens et al., 2003b). As a result, each voxel in the Broca's mask had four associated connectivity indices, indicating the number of probabilistic streamlines connecting that voxel to each of the four targets. We parcellated the Broca's area mask to assign each seed voxel in the mask to one of the medial cortical targets based on the highest connectivity index..

Seeding again from these parcellated sub-regions we calculated new probabilistic tractography streamlines between each voxel in the Broca's area sub-regions and each medial frontal target separately. Resulting connectivity distributions were truncated to exclude voxels having fewer than 1% of the maximum number of streamlines originating within the parcellated seed mask, which number varied across target masks and across participants. Post-parcellation tractography is reported in the Results section.

Seed and target masks for tractography

The masks of Broca's area were drawn on the structural scan of each subject in the native acquisition space. The lateral-most sagittal slice of the frontal cortex of the skull-stripped structural scan was used as the lateral border of each Broca's area mask. The medial border was 10 mm from the lateral border. The Broca's mask's dorsal border was the inferior frontal sulcus, while the ventral border was the Sylvian fissure. The Broca's mask's anterior border was defined by a coronal plane through the anterior margin of the anterior horizontal ramus of the Sylvian fissure, and its posterior border was inferior precentral sulcus. To define the target regions in medial frontal cortex, the skull-stripped structural scans of each participant were normalized to the Talairach atlas (Talairach & Tournoux, 1988) using AFNI (Cox 1996). The coronal plane perpendicular to the anterior commissure - posterior commissure (AC-PC) line, and tangent to the AC caudally in the most medial slice of the left hemisphere, was used to divide Pre-SMA from SMA within BA 6 (Picard & Strick, 2001). The caudal border of SMA was located 20 mm posterior to this division. The rostral border of Pre-SMA was defined to be 20 mm anterior to this division. Medial BA 8 was defined as extending 20 mm anteriorly from the rostral border of Pre-SMA. The caudal border of BA 9 began just anterior to the rostral border of BA 8, while the rostral border of BA 9 was drawn 20 mm anterior to its caudal border. All medial frontal masks were drawn to be non-overlapping and extended 7 slices (~7 mm) laterally from the medial extent of the left hemisphere in the Talairach space. The cingulate sulcus served as the inferior border for

each of the medial frontal masks, with the crest of the brain as the superior border. The inferior border of the BA 9 mask was defined by a line connecting the genu of the corpus callosum with the genu of the cingulate sulcus, projecting anteriorly where the cingulate sulcus was no longer inferior to BA 9. Each of the medial frontal target masks was back-transformed from Talairach space into the participant's native acquisition space, and each mask was then registered to the participant's diffusion space using the linear transform generated by the registration of the participant's structural scan to their diffusion scan (using FSL's FLIRT).

Exclusion masks for tractography

To prevent potential inclusion of the U-shaped short association fibers connecting inferior frontal gyrus to adjacent gyri, exclusion masks were drawn contiguous to Broca's area seed masks to exclude posterior precentral gyrus and superior-anterior middle frontal gyrus. Exclusion masks were also drawn in the corpus callosum and internal capsule to exclude crossing or descending motor projections.

Analysis of Surrogate data

To evaluate whether these methods would artifactually influence the inferred anatomy of our participants we created a surrogate data set (Theiler et al., 1992). First, we generated a 4-dimensional array (X, Y, Z, Gradient Direction) having the geometry of brain-only voxels from participant #1 (Smith, 2002). Next, we inserted random Gaussian noise in each array cell (surrogate voxel). We scaled the resulting noise-only surrogate data to match the range of signal intensities of the participant's brain image. Next, we estimated diffusion parameters of these surrogate data using MCMC (Behrens et al., 2007). We re-ran our tractography analysis using the same seed, termination, and exclusion masks to trace fibers between Broca's area and the medial frontal cortex, as though the surrogate data were a brain image rather than random noise. Furthermore, we used the central voxel of the Broca's area mask to trace projections originating from this location without applying any additional restrictions. Zero projections resulted from applying our original method to the random noise surrogate data. Inferred "tracts" from the central voxel tracing dispersed only a short distance (< 10 voxels) from the starting location.

Results

Visualization of connectivity-based parcellation of Broca's area, shown in Figure 1, shows generally anterior-to-posterior ordered connectivity. Anterior portions of Broca's area showed the highest likelihood of connection with anterior medial cortex (BA 9 and/or BA 8, light green and dark green respectively), whereas the most posterior portions of Broca's area typically have posterior medial cortex as their most likely targets for connection (Pre-SMA and/or SMA, blue and orange respectively).

Overall, BA 8 and 9 dominate connectivity in more than 50% of Broca's area in seven of nine participants (i.e., except for participants 5 and 7). Relatively few voxels in Broca's area in any of the participants showed high likelihoods of connection with SMA. For our five youngest participants (1, 2, 3, 4, 5), aged 22 to 65 years, no voxel in Broca's area exhibited an SMA connectivity index higher than those of the remaining targets in medial frontal cortex. For these five participants, Broca's area parcellated into only three connectivity regions: BA 9, 8, and Pre-SMA. The absence of SMA in Broca's area parcellation with the present analysis does not suggest that Broca's area – SMA connectivity does not exist, but rather that SMA has a lower connectivity index compared to the other three areas in the medial frontal cortex. Based on the previous macaque tracer studies of connectivity between ventral lateral premotor cortex and SMA, if we had included ventral lateral BA 6 and BA 47

in our analysis to determine connectivity of the larger Broca's region, rather than the smaller BA 44/45 Broca's area, then stronger connectivity with the SMA would be expected (Ghosh and Gattera, 1995). Parcellation-based connectivity between Broca's area and SMA was more evident for the oldest four out of nine of our participants (6, 7, 8, 9), aged 70 to 82 years.

Given that the subjects with and without SMA represented in the Broca's area parcellation were so clearly divided on the basis of age, a Mann-Whitney *U* test was applied to determine if there was a difference in the rank order of ages between those groups. The results indicate that participants without SMA representation are significantly younger than those with SMA representation, $U = 0$, $p = 0.016$ (two-tailed). This finding is consistent with an anterior-to-posterior gradient of white matter decline (e.g., Corchesne, et al. 2000) accelerated past age 65 (Westlye, et al., 2010), which could in principle more strongly affect BA 9, 8, and pre-SMA, thus allowing low SMA connectivity to achieve greater relative prominence. It also should be noted that participant 7 in Figure 1 showed no parcellation for Pre-SMA.

Using probabilistic tractography, we traced inferred fiber bundles connecting Broca's area to each of the four medial frontal targets. Figure 2 shows an array of 3D representations of these fibers for each of our nine participants. Fiber orientation and trajectory follow a clear anterior-posterior trend, where more anterior portions of the Broca's area project to BA 9 and 8 (yellow and green respectively) and more posterior portions of Broca's area project to Pre-SMA and SMA (blue and orange respectively). The five younger participants who did not show any high-likelihood connections between Broca's area and SMA with connectivity-based parcellation (shown in Figure 1) accordingly lack corresponding inferred fibers with probabilistic tractography, shown in Figure 2. The four older participants in whom connectivity-based parcellation was revealed Broca's area and SMA (Figure 1) also revealed inferred fibers with probabilistic tractography (Figure 2).

Discussion

Structural connectivity of Broca's area and potential functional implications thereof have been the topic of many previous studies. It has been shown that Broca's area interconnects with the inferior parietal lobule, and the superior and middle temporal gyri (Catani et al., 2001; Glasser & Rilling, 2008; Frey et al., 2008), consistent with classical models of language. However, other cortical regions have yet to be shown as projection sites of human Broca's area (BA 44/45). The present paper examines Broca's area connectivity with medial frontal cortex using diffusion-weighted MRI, probabilistic tractography, and connectivity-based parcellation. Connectivity between these regions exists in non-human primates; macaque's BA 44 and 45 were shown to connect to BA 6, 8, and 9 in medial frontal cortex (Petrides & Pandya, 2002). Cross-species generality between BA 44 and 45 connectivity in macaque and Broca's area connectivity in humans was recently demonstrated by separate fiber pathways connecting BA 45 to STG and BA 44 to inferior parietal lobule in macaque which also were shown to be present in human (Frey et al., 2008). Based on these findings, we hypothesized that medial frontal connectivity of BA 44 and BA 45 found in macaque would generalize to Broca's area medial frontal connectivity in humans. To our knowledge, we are the first to show structural connections between Broca's area and BA 6, 8, and 9 in human medial frontal cortex. With the exception of connections between SMA and Broca's area, the present findings were consistent across our subjects regardless of their ages.

Although the present study used a moderate number of diffusion-gradient directions, the signal-to-noise ratio of the brain images was sufficient to represent underlying anatomy. Null results from analysis of the random noise surrogate data clearly show that neither the brain images anterior-to-posterior gradient in connectivity-based parcellation, nor

trajectories of the inferred tracts, arise artifactually from our methods. If that were the case, then surrogate data could produce similar results as the brain images, and this did not occur.

When examining the overall strength of connectivity between Broca's area and the four regions of interest in the medial frontal cortex we note that our findings indicate that for five of our participants parcellation-based connectivity between Broca a area and SMA was very sparse. For these five participants parcellation maps of Broca's area contain only three sub-regions showing the highest likelihood of projection to Pre-SMA, BA 8, and BA 9 (Figure 1, participants 1, 2, 3, 4, and 5). For the other four participants, the sub-region of Broca's area showing highest connectivity to SMA is much smaller compared to sub-regions with highest connectivity to Pre-SMA, BA 8, and BA 9. Previous macaque tracer studies show extensive connectivity between SMA and the ventral lateral BA 6 of primate motor cortex (Ghosh and Gattera, 1995;Dancase et al., 2007). Based on these results from macaque, we believe that expansion of our region of interest to include ventral lateral BA 6 and BA 47, so as to constitute Broca's region as described by Hagoort and colleagues, would result in stronger connectivity with SMA (Hagoort, 2006). Changes in the SMA connectivity could reflect age of the participants. Participants who did show SMA connectivity based on parcellation of Broca's area were older (70 to 82 years of age) than those who did not show SMA connectivity (22 to 65). Age-related deterioration in white matter as measured by fractional anisotropy (e.g., Salat et al., 2006; Westlye, et al., 2010) or volumetry (e.g., Corchesne et al., 2000; Westlye, et al. 2010) has been previously reported to affect the prefrontal or more anterior cortex to a larger extent than other, more posterior cortical areas. Thus, reduced integrity of white matter connecting Broca's area more strongly affecting anterior portions of the medial frontal cortex as compared with more posterior SMA, could potentially explain the relatively increased prominence of SMA connectivity in Broca's area parcellations in the four oldest participants. However, formal analysis of this trend is made difficult by our small sample size. Further studies investigating potential age effects on connectivity of Broca's area and the prefrontal cortex should be carried out to fully understand changes in these white matter fiber tracts with age.

Previous work on connectivity-based parcellation of Broca's area by Anwander and colleagues seems to follow known anatomical landmarks delineating BA 44 and 45. In particular, in the six participants they examined, the anterior ascending ramus of the Sylvian fissure fairly consistently demarcated the border of connectivity-parcellated BA 44 and 45 (see Figure 4, page 820 Anwander et al., 2007). In five out of nine of the present participants, voxels showing the highest connectivity index with Pre-SMA are located posterior to the anterior ascending ramus (younger participants 1, 3, and older participants 4, 5, 8. In all of our participants, voxels with the highest connectivity index with BA 9 are located predominantly posterior to the anterior ascending ramus, with only a few voxels anterior to it. Voxels that have high connectivity index with BA 8 are located anterior to the anterior ascending ramus in seven out of nine participants (younger participant 2, 3, and older participants 4, 5, 6, 7, 9), and for the other two these voxels are distributed both posteriorly and anteriorly to the anterior ascending ramus (younger participant 1, older participant 8). Individual differences in location of connectivity-based sub-regions within Broca's area are not surprising given previous histological work on intersubject variability of BA 44 and 45 (Amunts et al., 1999). Amunts and colleagues have shown that although in some hemispheres the border between BA 44 and 45 is defined by the anterior ascending ramus of the Sylvian fissure, in others it is located close to the diagonal sulcus, or interposed between these two sulci. Apparent disagreements between borders defined by anatomical landmarks, connectivity or histology may reflect factors such as brain size, heredity and life experiences.

What does the presently described anterior-posterior connectivity gradient between medial frontal cortex and Broca's area suggest for involvement of medial frontal cortex in language? Numerous studies have shown anterior-posterior functional organization of Broca's area, wherein more anterior portions corresponding to BA 45 are implicated in semantic processing, while more posterior portions corresponding to BA 44 are involved in phonological and syntactic processing (Amunts et al., 2004; Hagoort, 2006). Using a verbal fluency task in conjunction with cytoarchitectonic probabilistic maps of BA 44 and 45 suggests that the left BA 45 is involved in semantic aspects of language processing, whereas BA 44 is implicated in speech programming (Amunts et al., 2004). Using a similar approach, Binkofski and colleagues implicated BA 44 in the mediation of higher-order forelimb movement control (Binkofski et al., 2000). Support for this functional delineation also comes from positron emission tomography studies using the combination of probabilistic cytoarchitectonic maps and functional activation (Horwitz, et al., 2003) in which activation in BA 44 was attributed to non-linguistic, laryngeal or limb motor production in speech or sign language. Thus, based on our findings, one plausible implication of the current data is that (a) given the anterior-posterior connectivity patterns between Broca's area and medial frontal cortex then (b) a similar functional gradient might be found in medial frontal areas. Piccard and Strick in their work on SMA and Pre-SMA have shown that connectivity of a region defines its function (Piccard & Strick, 2001). Medial frontal cortex has been previously implicated to be involved in initiation of cognitive aspects of spontaneous language (Nielson & Jacobs, 1951; Barris & Schuman, 1953; Luria, 1966; Tijssen et al., 1984). fMRI during phonetic and semantic analysis of aurally presented stimuli indicated extensive activation of BA 8/9/10 as well as Pre-SMA during the semantic decision task, whereas activation of the SMA was found only when the subjects were asked to attend to characteristics of non-linguistic stimuli (Binder et al., 1997). Lesions to the SMA/Pre-SMA complex have been reported to induce word finding difficulties in speech (Jonas, 1981). Crosson and colleagues have also demonstrated with fMRI that Pre-SMA is involved in internally guided word generation (Crosson et al., 2001). fMRI activation of SMA is also seen during volitional expiration, which could suggest involvement of this region in control of vocalizations (Ramsay et.a., 1993). Letter/character finding is also attributed to Pre-SMA by an fMRI study in which participants had to find correct Kanji characters to solve a puzzle (Matsuo et al., 2001). A meta-analysis by Picard and Strick (1996), examining functional activation patterns of SMA and Pre-SMA, suggests that SMA is involved in simple speech tasks including simple repetition and overpracticed verbal associations, whereas Pre-SMA is involved in more complex verbal tasks, such as word production in new conditional associations. Functional organization of medial frontal cortex does seem to follow to some extent an anterior-posterior gradient similar to that of Broca's area. Data from our own laboratory (Crosson et al., 2003) suggests that the story has at least one more factor. Word generation data from this latter study were relatively consistent with the anterior to posterior gradient for lateral cortices. Specifically, when subjects generated words as exemplars of categories (semantic processing), cortex along the inferior frontal sulcus was active; and when subjects generated words that rhymed with the given word (phonological processing), premotor cortex along the precentral sulcus was active (Broca's region, expanded posteriorly). However, pre-SMA was active when words were generated from either a semantic category or a rhyming cue (lexical but non-semantic). Pre-SMA was not active when nonsense syllables were generated from beginning and ending consonant blends. Hence, Pre-SMA was active when generation involved lexical items, which have pre-existing representations in the brain, but not active when generation involved non-lexical and non-semantic novel phonological items (nonsense syllables). Clearly the role of lexical and non-lexical processing (as well as semantic, phonological, and syntactic processing) should be taken into account in future investigations of the functional relationships linking medial frontal cortex and Broca's area.

The current study has some limitations. The participant sample is too small to identify age-related or gender-related effects. Like other applications of magnetic resonance imaging the signals are acquired through volume and time averaging, which sets limits on resolution and allows for degradation by unwanted head motion. The present approach of selecting connectivity candidates based on high empirical probability densities of Markov Chain Monte Carlo streamlines cannot rule out overlapping or parallel connections. Unlike high-resolution techniques of stains transported through neurons, DW-MRI infers structure (but it is also noninvasive).

Gender differences in neural architecture have been previously investigated using fMRI (Shaywitz et al., 1995), as well as, DW-MRI (Sullivan et al., 2010; Hsu et al., 2008). Our sample consisting of seven females and two males did not allow us to investigate gender differences in Broca's area and medial frontal cortex connectivity. Further studies including larger sample sizes and gender-balanced groups of participants are necessary to definitively determine the presence or absence of gender related differences in the structural connectivity in question.

Our findings indicate that subjects without SMA representation in their Broca's area parcellation are younger than those with SMA representation. The limited number of participants in our study prevents us from carrying out a more elaborate formal statistical comparison of age related differences in the connectivity patterns between Broca's area and the medial frontal cortex. Future studies investigating changes in the integrity of the white matter connecting Broca's area and the prefrontal cortex to medial frontal cortex would be crucial in determining the underlying causes of the potential age related differences that could not be addressed extensively in the present manuscript.

Inferred structural connectivity was presently guided by anatomical landmarks to define Broca's area and regions within medial frontal cortex. As mentioned above, anatomical landmarks and cytoarchitectonic boundaries often do not agree (Amunts et al., 1999). Functional parcellation provides a more precise definition of neuroanatomy specific to each participant's functional organization, as demonstrated by Amunts and colleagues (Amunts et al., 2004). Thus, it is critical that future studies should incorporate fMRI and related functional modalities to better delineate functional sub-regions within both Broca's area and medial frontal cortex (Amunts & Zilles, 2001; Horwitz et al., 2003; Eickhoff et al., 2006). The functional information could improve our understanding of how and when a particular pathway in the Broca's - medial frontal network is used.

Furthermore, it is crucial to determine whether anterior Broca's area co-activates synchronously with anterior medial frontal cortex, and posterior Broca's area co-activates with posterior medial frontal cortex, consistent with the anterior-posterior connectivity patterns demonstrated in the present study. Partial support for this hypothesis can be found in work by Kouneiher and colleagues, who showed functional connectivity between the posterior lateral prefrontal cortex, including BA 44/45 and posterior medial frontal cortex (Pre-SMA) on trials evoking contextual motivation (Kouneiher et al., 2009). Future studies implementing methods similar to those of Kouneiher et al. using language tasks will provide further insights into functional organization of the Broca's - medial frontal cortex networks. A further challenge for future studies might be to expand Broca's area into Broca's region, which includes ventral lateral BA 6 and pars orbitalis (BA 47) (Hagoort, 2006) in addition to pars triangularis (BA 45) and pars opercularis (BA 44), the latter two being traditional Broca's area.

Acknowledgments

This material is based upon work supported by the Office of Research and Development (Rehabilitation R&D Service, Center of Excellence grant #F2182C and Senior Research Career Scientist award #B6364L) to Crosson, Department of Veterans Affairs and by grant # R01 DC007387 to Crosson.

References

1. Amunts K, Weiss PH, Mohlberg H, Pieperhoff P, Gurd J, Shah JN, et al. Analysis of the neural mechanisms underlying verbal fluency in cytoarchitectonically defined stereotaxic space – The role of Brodmann's areas 44 and 45. Neuroimage 2004;22:42–56. [PubMed: 15109996]
2. Amunts K, Zilles K. Advances in cytoarchitectonic mapping of the human cerebral cortex. Neuroimaging Clin N Am 2001;11(2):151–69. vii. [PubMed: 11489732]
3. Amunts K, Schleicher A, Burgel U, Mohlberg H, Uylings HBM, Zilles K. Broca's region revisited: cytoarchitecture and intersubject variability. Journal of Comparative Neurology 1999;412:319–341. [PubMed: 10441759]
4. Anwander A, Tittgemeyer M, von Cramon DY, Friederici AD, Knosche TR. Connectivity-based parcellation of Broca's area. Cereb Cortex 2007;17(4):816–825. [PubMed: 16707738]
5. Barris RW, Schuman HR. Bilateral anterior cingulate gyrus lesions: syndrome of the anterior cingulate gyri. Neurology 1953;3:44–52. [PubMed: 13013498]
6. Basser PJ, Mattiello J, LeBihan D. MR diffusion tensor spectroscopy and imaging. Biophys J 1994;66(1):259–267. [PubMed: 8130344]
7. Behrens TEJ, Johansen-Berg H, Jbabdi S, Rushworth MFS, Woolrich MW. Probabilistic diffusion tractography with multiple fibre orientations: What can we gain? NeuroImage 2007;34(1):144–155. [PubMed: 17070705]
8. Behrens TEJ, Johansen-Berg H, Woolrich MW, Smith SM, Wheeler-Kingshott CAM, Boulby PA, Barker GJ, Sillery EL, Sheehan K, Ciccarelli O, Thompson AJ, Brady JM, Matthews PM. Non-invasive mapping of connections between human thalamus and cortex using diffusion imaging. Nature Neurosci 2003b;6:750–757. [PubMed: 12808459]
9. Behrens TEJ, Woolrich MW, Jenkinson M, Johansen-Berg H, Nunes RG, Clare S, Matthews PM, Brady JM, Smith SM. Characterization and propagation of uncertainty in diffusion-weighted MR imaging. Magn Reson Med 2003a;50:1077–1088. [PubMed: 14587019]
10. Binder JR, Frost JA, Hammeke TA, Cox RW, Rao SM, Prieto T. Human brain language areas identified by functional magnetic resonance imaging. J Neurosci 1997;17(1):353–362. [PubMed: 8987760]
11. Binkofski F, Amunts K, Stephan KM, Posse S, Schormann T, Freund HJ, Zilles K, Seitz RJ. Broca's region subserves imagery of motion: a combined cytoarchitectonic and fMRI study. Hum Brain Mapp 2000;11:273–285. [PubMed: 11144756]
12. Binkofskii F, Amunts K, Stephan KM, Posse S, Schormann T, Freund HJ, Zilles K, Seitz RJ. Broca's region subserves imagery of motion: A combined cytoarchitectonic and fMRI study. Human Brain Mapping 2000;11(4):273–285. [PubMed: 11144756]
13. Broca P. Remarques sur le siège de la faculté du langage articulé; suivies d'une observation d'aphemie. Bull Soc Anat Paris 1861;6:330–357.
14. Catani M, Jones DK, Ffytche DH. Perisylvian language networks of the human brain. Ann Neurol 2005;57(1):8–16. [PubMed: 15597383]
15. Ciccarelli O, Behrens TEJ, Altmann DR, Orrell RW, Howard RS, Johansen-Berg H, Miller DH, Matthews PM, Thompson AJ. Probabilistic diffusion tractography: a potential tool to assess the rate of disease progression in amyotrophic lateral sclerosis. Brain 2006;129(7):1859–1871. [PubMed: 16672290]
16. Courchesne E, Chisum HJ, Townsend J, Cowles A, Covington J, Egaas B, Harwood M, Hinds S, Press GA. Normal brain development and aging: quantitative analysis at in vivo MR imaging in healthy volunteers. Radiology 2000;216:672–682. [PubMed: 10966694]
17. Cox RW. AFNI software for analysis and visualization of functional magnetic resonance neuroimages. Comput Biomed Res 1996;29:162–173. [PubMed: 8812068]

18. Crosson B. Subcortical mechanisms in language: lexical–semantic mechanisms and the thalamus. Brain Cogn 1999;40(2):414–438. [PubMed: 10413568]
19. Crosson B, Benefield H, Cato MA, Sadek JR, Moore AB, et al. Left and right basal ganglia and frontal activity during language generation: Contributions to lexical, semantic, and phonological processes. J Int Neuropsychol Soc 2003;9:1061–1077. [PubMed: 14738287]
20. Crosson B, McGregor K, Gopinath KS, Conway TS, Benjamin M, Chang YL, Moore AB, Raymer AM, Briggs RW, Sherod MG, Wierenga CE, White KD. Functional MRI of language in aphasia: a review of the literature and the methodological challenges. Neuropsychol Rev 2007;17(2):157–177. [PubMed: 17525865]
21. Crosson B, Sadek JR, Maron L, Gokcay D, Mohr CM, Auerbach EJ, Freeman AJ, Leonard CM, Briggs RW. Relative shift in activity from medial to lateral frontal cortex during internally versus externally guided word generation. J Cogn Neurosci 2001;13(2):272–283. [PubMed: 11244551]
22. Dancause N, Barbay S, Frost SB, Mahnken JD, Nudo RJ. Interhemispheric connections of the ventral premotor cortex in a new world primate. Journal of Comparative Neurology 2007;505(6):701–715. [PubMed: 17948893]
23. Eickhoff SB, Amunts K, Mohlberg H, Zilles K. The Human Parietal Operculum. II. Stereotaxic Maps and Correlation with Functional Imaging Results. Cerebral Cortex 2006;16(2):268–279. [PubMed: 15888606]
24. Frey S, Campbell JSW, Pike GB, Petrides M. Dissociating the human language pathways with high angular resolution diffusion fiber tractography. Journal Neurosci 2008;28(45):11435–11444.
25. Friedrici A. Pathways to language: fiber tracts in the human brain. Trends in Congtinive Sciences 2009;13(4):175–181.
26. Ghosh S, Gattera R. A comparison of the ipsilateral cortical projections to the dorsal and ventral subdivisions of the macaque premotor cortex. Somatosent Mot Res 1995;12:359–378.
27. Glasser MF, Rilling JK. DTI tractography of the human brain's language pathways. Cereb Cortex 2008;18(11):2471–2482. [PubMed: 18281301]
28. Hagoort, P. On Broca, Brain, and Binding. In: Grodzinsky, Y.; Amunts, K., editors. Broca's region. Oxford UP; New York: 2006.
29. Horwitz B, Amunts K, Bhattacharyya R, Patkin D, Jeffries K, Zilles K, Braun AR. Activation of Broca's area during the production of spoken and signed language: a combined cytoarchitectonic mapping and PET analysis. Neuropsychologia 2003;41(14):1868–1876. [PubMed: 14572520]
30. Horwitz B, Rumsey JM, Donohue BC. Functional connectivity of the angular gyrus in normal reading and dyslexia. PNAS 1998;95(15):8939–8944. [PubMed: 9671783]
31. Hsu J, Leemans A, Bai C, Tsai Y, Chiu H, Chen W. Gender differences and age-related white matter changes of the human brain: A diffusion tensor imaging study. Neuroimage 2007;39(2):566–577. [PubMed: 17951075]
32. Jenkinson M, Smith SM. A global optimisation method for robust affine registration of brain images. Med Image Anal 2001;5(2):143–156. [PubMed: 11516708]
33. Jonas S. The supplementary motor region and speech emission. J Commun Disord 1981;14:349–373. [PubMed: 7287912]
34. Klein D, Milner B, Zatorre RJ, Meyer E, Evans AC. The neural substrates underlying word generation: a bilingual functional-imaging study. PNAS 1995;92(7):2899–2903. [PubMed: 7708745]
35. Kouneiher F, Charron S, Koechlin E. Motivation and cognitive control in the human prefrontal cortex. Nature Neurosci 2009;12:939–945. [PubMed: 19503087]
36. Lichtheim L. On aphasia. Brain 1885;7:433–484.
37. Luria, AR. Human brain and psychological processes. Harper & Row; New York: 1996.
38. Nielsen JM, Jacobs LL. Bilateral lesions of the anterior cingulated gyri: report case. Bull LA Neurol Soc 1951;16:231–234.
39. Nielsen JM, Jacobs LL. Bilateral lesions of the anterior cingulate gyri; report of case. Bull Los Angeles Neurol Soc 1951;16:231–234. [PubMed: 14839354]
40. Petrides M. A functional organization of the human frontal cortex for mnemonic processing: evidence from neuroimaging studies. Ann NY Acad Sci 1995;769:85–96. [PubMed: 8595046]

41. Petrides M. Lateral prefrontal cortex: architectonic and functional organization. Phil Trans R Soc B 2005;360(1456):781–795. [PubMed: 15937012]
42. Petrides, M.; Pandya, DN. Comparative architectonic analysis of the human and the macaque frontal cortex. In: Boller, F.; Grafman, J., editors. Handbook of Neuropsychology. Vol. 9. Elsevier; Amsterdam: 1994. p. 17-589.
43. Petrides M, Pandya DN. Comparative cytoarchitectonic analysis of the human and the macaque ventrolateral prefrontal cortex and corticocortical connection patterns in the monkey. Eur J Neurosci 2002;16:291–310. [PubMed: 12169111]
44. Picard N, Strick PL. Medial wall motor areas: a review of their location and functional activation. Cereb Cortex 1996;6:342–353. [PubMed: 8670662]
45. Ramsay SC, Adams L, Murphy K, et al. Regional cerebral blood flow during volitional expiration in man: a comparison with volitional inspiration. J Physiol 1993;461:85–101. [PubMed: 8350282]
46. Ridderinkhof KR, Ullsperger M, Crone EA, Nieuwenhuis S. The role of the medial frontal cortex in cognitive control. Science 2004;306(5695):443–447. [PubMed: 15486290]
47. Rizzolatti G, Arbib MA. Language within our grasp. Trends Neurosci 1998;21(5):188–194. [PubMed: 9610880]
48. Rizzolatti G, Craighero L. The mirror-neuron system. Annu Rev Neurosci 2004;27:169–192. [PubMed: 15217330]
49. Rushworth MFS, Buckley MJ, Behrens TEJ, Walton ME, Bannerman DM. Functional organization of the medial frontal cortex. Curr Opin Neurobiol 2007;17(2):220–227. [PubMed: 17350820]
50. Rushworth MFS, Walton ME, Kennerley SW, Mannerman DM. Action sets and decisions in the medial frontal cortex. Trends Cogn Sci 2004;8(9):410–417. [PubMed: 15350242]
51. Salat DH, Tuch DS, Hevelone ND, Fischl B, Corkin S, Rosas HD, Dale AM. Age-related changes in prefrontal white matter measures by diffusion tensor imaging. Annals of New York Academy of Sciences 2006;1064 :37–49.
52. Shaywitz BA, Shaywitz SE, Pugh KR, Constable RT, Skudlarski P, Fulbright RK, Bronen RA, Fletcher JM, Shankweiler DP, Katz L, Gores JC. Sex differences in the functional organization of the brain for language. Nature 1995;373:607–609. [PubMed: 7854416]
53. Smith M. Fast robust automated rain extraction. Human Brain Mapping 2002;17(3):143–155. [PubMed: 12391568]
54. Sullivan EV, Rohlfing T, Pfefferbaum A. Quantitative fiber tracking of the lateral and interhemispheric white matter systems in normal aging: Relations to timed performance. Neurobiology of Aging 2010;31(3):464–481. [PubMed: 18495300]
55. Talairach, J.; Tournoux, P. Co-planar stereotaxic atlas of the human brain. 1988.
56. Theiler, J.; Eubank, S.; Longtin, A.; Galdrikian, B.; Farmer, JD. Physica D. Vol. 58. Thieme; Stuttgart, Germany: 1992. Testing for nonlinearity in time series: The method of surrogate data.
57. Tijssen CC, Tavy DLJ, Hekster REM, Bots GTAM, Endtz LJ. Aphasia with a left frontal interhemispheric hematoma. Neurology 1984;34:1261–1264. [PubMed: 6540417]
58. Wernicke, C. Der aphasische Symptomenkomplex. Breslau; Cohn, Weigert: 1874.
59. Westlye LT, Walhovd KB, Dale AM, Bjornerud A, Due-Tonnessen P, Engvig A, Grydeland H, Tammes CK, Ostby Y, Fjell AM. Life-span changes in the human brain white matter: diffusion tensor imaging and volumetry. Cerebral Cortex. 2009 in press.

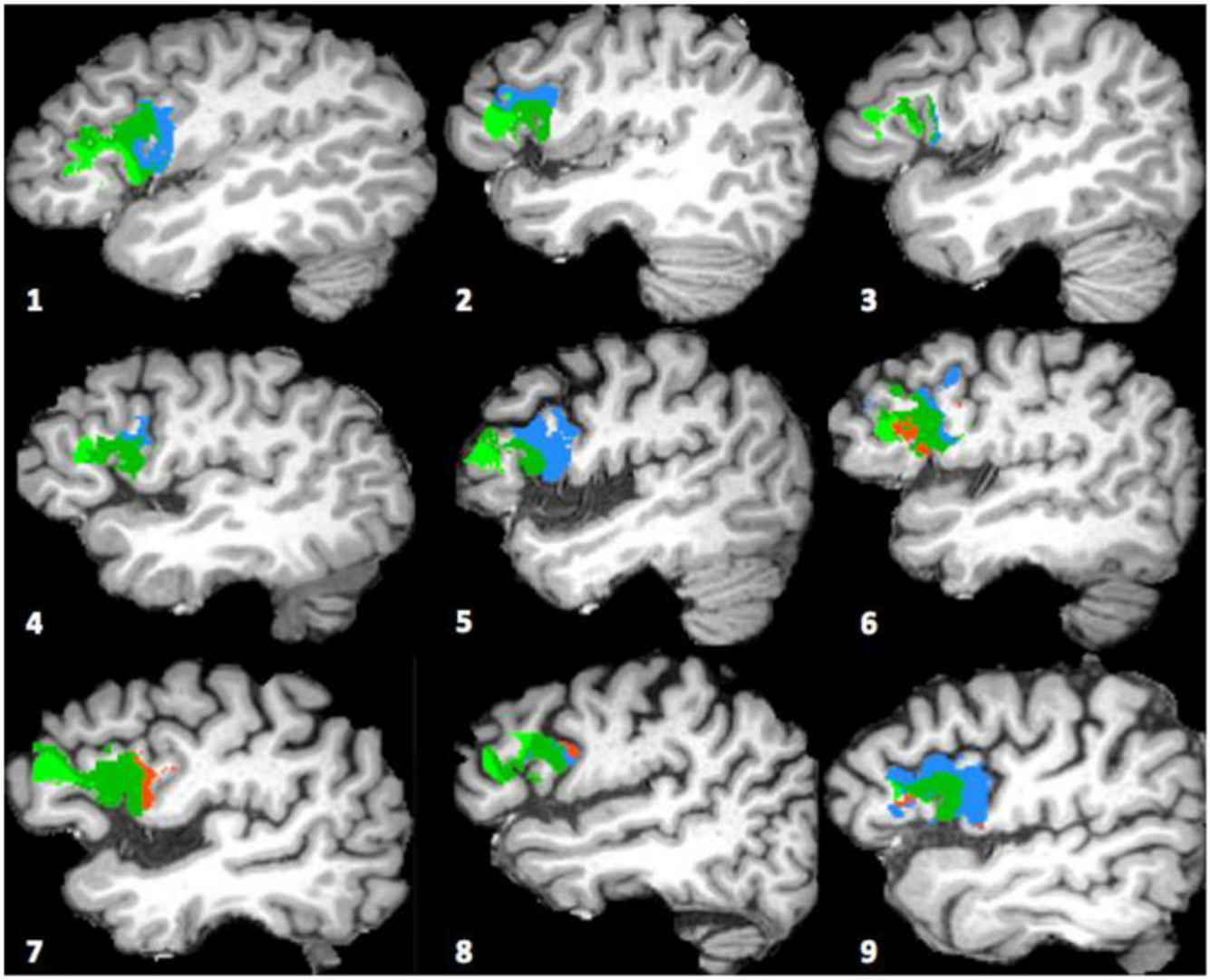

Figure 1.
Connectivity-based parcellation of Broca's area. Light green: BA 9; dark green: BA 8; blue: Pre-SMA; orange: SMA.

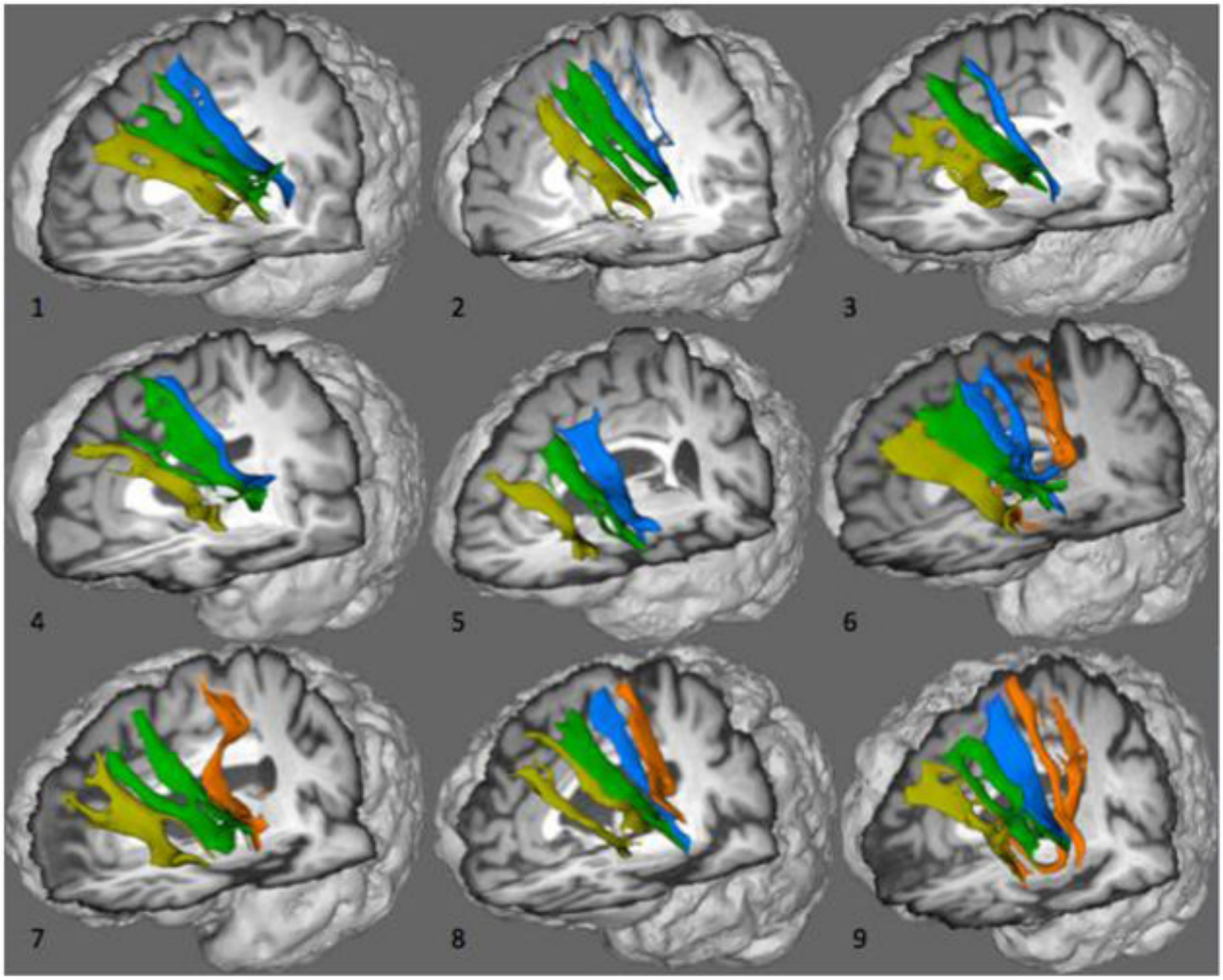

Figure 2.
White matter tracts inferred by probabilistic tractography connecting Broca's area (BA 44/45) and medial frontal cortex. Yellow: BA 9; dark green: BA 8; blue: Pre-SMA; orange: SMA. Images obtained from participants indicated by the same number in Table 1.

Table 1

Age, gender, and education history of the participants.

Participant ID	Age	Gender	Years of Education
S1	22	F	16
S2	25	M	16
S3	32	F	16
S4	64	F	16
S5	65	F	14
S6	70	F	16
S7	74	F	13
S8	81	M	20
S9	82	F	18